# Primary aragonite and high-Mg calcite in the late Cambrian (Furongian). Potential evidence from marine carbonates in Oman.

**Joyce E. Neilson, Alexander T. Brasier and Colin P. North**

Department of Geology and Petroleum Geology, University of Aberdeen, Aberdeen, AB24 3UE, U.K.

Corresponding author: Joyce Neilson, j.neilson@abdn.ac.uk, +44 (0)1224 273457

Running Title: Aragonite and HMC in the late Cambrian.

## Abstract

Transient aragonite seas occurred in the early Cambrian but several models suggest the late Cambrian was a time of calcite seas. Here, evidence is presented from the Andam Group, Huqf High, Oman (Gondwana) that suggests a transient Furongian (late Cambrian) aragonite sea, characterized by the precipitation of aragonite and high-Mg calcite ooids and aragonite isopachous, fibrous, cements. Stable carbon isotope data suggest that precipitation occurred just before and during the SPICE (Steptoean Positive Carbonate Isotope Excursion). Aragonite and high-Mg calcite precipitation can be accounted for if mMg:Ca ratios were around 1.2 given the very high atmospheric $CO_2$ at that time and if precipitation occurred in warm waters associated with the SPICE. This, together with reported occurrences of early Furongian aragonite ooids from various locations in North America (Laurentia), suggests that aragonite and high-Mg calcite precipitation from seawater may have been more than just a local phenomenon.


## Introduction

Seawater chemistry has varied over geological time: Phanerozoic oceans are characterized as being either 'aragonitic', with inorganic aragonite and high-Mg calcite (HMC) precipitation, or 'calcitic', with inorganic low-Mg calcite (LMC) precipitation (e.g. Sandberg, 1983; Demicco et al., 2005). The mMg:Ca ratio of seawater is believed to have played a major role in this process; ratios >2 are often cited as favouring aragonite seas, ratios <2 favouring calcite seas (e.g. Füchtbauer and Hardie, 1976, 1980, Ries, 2009, Balthasar and Cusack, 2015 and Figure 1). Temperature and $pCO_2$ however have also been shown to have

an effect (e.g. Sandberg, 1983, Burton and Walter, 1987, Morse et al., 1997, Balthasar and Cusack, 2015, Lee and Morse, 2010).

Balthasar and Cusack (2015) and Kiessling (2015) concluded that the boundary between aragonite-calcite seas is poorly constrained; 'gray' (Balthasar and Cusack, 2015) and 'fuzzy' (Kiessling, 2015). Kiessling (2015) suggested that "calcite, aragonite and gray [overlapping] states must be better constrained in time and space. Little progress has been made quantifying the proportional mineral abundance in oolites and cements since the mid-1980's".

The early Cambrian was characterized by alternating intervals of aragonite and calcite seas (Table 1). Zhuravlev and Wood (2008) indicate that from Stage 5 onwards into the Ordovician, inorganic cements and ooids precipitated from seawater were composed of LMC. However, here data are presented from the Al Bashair Formation of the Andam Group, Oman, along with a synthesis of published data from elsewhere, which suggest that some inorganic precipitates may have been composed of aragonite and HMC during the early Furongian (Tables 1, 2), coincident with the SPICE which is believed to represent a widespread ocean anoxic event (e.g. Brasier, 1993, Saltzman, 2000, Gill et al., 2011).

## Geological Setting

The Lower Palaeozoic of Oman (Gondwana) exposed in the Huqf High, is represented by the Haima Supergroup comprising the Mahatta Humaid, Andam and Safiq Groups (Forbes et al., 2010). The late Cambrian lower Andam Group Al Bashair and Barik Formations (Table 1) are dominantly siliciclastic but the lower Al Bashair Formation (LAB of Al Marjibi, 2011) contains

55 many thin carbonate layers characterized by an open marine fauna (e.g. trilobite,
56 echinoderm and brachiopod fragments) along with glauconite. The LAB represents the first
57 major Cambrian marine incursion in the region following continental deposition of the
58 Miqrat Fm (Droste, 1997). A return to continental sedimentation is observed in the upper Al
59 Bashair Fm (UAB) and overlying Barik Fm which was deposited in a braid delta system
60 (Droste, 1997).

61 Vizan et al. (2009) dated the top of the Al Bashair Fm as late Cambrian (494 Ma) using
62 magnetostratigraphy, in agreement with the stratigraphic and palaeontological ages of
63 Droste (1997).

64

65 **Methods and Materials**

66 40 polished thin-sections were prepared and analyzed using standard petrographic and
67 Scanning Electron Microscopy (SEM) techniques to determine their composition, texture,
68 grainsize and diagenesis.

69 Back-scatter SEM (BSEM) was used to identify Sr-bearing minerals (e.g. celestine). Two
70 samples were analysed further using a Cameca ims-4f ion microprobe with a 5nA $^{16}O^-$ beam
71 accelerated at 15kV. Beam diameter was 15 µm, energy offset 75 V and the image field 25
72 µm. The analyses were calibrated using three internal standards and collected over 1 day
73 (negligible drift). Elemental concentrations were measured in ppm and mol % $MgCO_3$
74 calculated using the method in Dickson (2014).

75 Stable isotopic data (carbon and oxygen) were also obtained from 18 whole rock powdered
76 samples of oolitic and bioclastic grainstones and 2 carbonate cemented sandstones.

77 Samples were hand-drilled using a 0.3mm drill bit to produce 1 mg bulk powders (individual
78 grains were too small to separate). Samples were dissolved overnight in tubes containing
79 phosphoric acid (70 °C) and evolved $CO_2$ measured with an Analytical Precision AP 2003
80 Mass Spectrometer. Repeat analyses of NBS-18 and internal calcite standards were
81 generally better than ±0.2‰ for carbon and ±0.3‰ for oxygen.

82

83 **Results**

84 The LAB is a peritidal to open marine succession consisting of carbonates and siliciclastics
85 (Figure 2). The carbonate facies include oolitic grainstones (Figures 3 a-b), bioclastic
86 grainstones with glauconite (Figure 3c), stromatolitic limestones, flat pebble conglomerates
87 and finely crystalline dolomite, whereas the siliciclastics include terrestrial mudstones,
88 siltstones and fine sandstones (Figures 3 d-e). Pure carbonates gradually disappear in the
89 UAB but a few bioclastic sandstones and limestones are found (Figure 2).

90 Petrographic analysis shows that ooids are of two types – those that exhibit radial fibrous
91 fabrics (Figure 3a) and those that have been neomorphosed or display oomouldic porosity,
92 termed relict coated grains (Figures 3b, 4a). Radial fibrous grains are much smaller (median
93 size 300-350 µm) than relict coated grains (median size 650-700 µm, Figure 5). Oomouldic
94 porosity (Figures 3b, 4) may be open, partially or totally filled by sparry calcite or celestine
95 cements (Figure 4a).

96 Radial ooids exhibit a darker shade of grey using BSEM imaging (Figure 4c) and contain local
97 microdolomite inclusions (Figure 4d). Ion microprobe analysis (Figure 7) revealed
98 concentrations of 1.19 – 1.91 mol % $MgCO_3$ (equivalent to 2866 – 4599 ppm Mg, Figure 8a)

with one value of 7.83 mol % $MgCO_3$ (19,032 ppm Mg). Mg concentrations in coeval echinoderm fragments are slightly higher (1.54 – 2.93 mol % $MgCO_3$, equivalent to 3716 – 5750 ppm Mg). Sr concentrations in the radial ooids range from 271-381 ppm, similar to the echinoderm fragments (303-387 ppm). Neomorphosed coated grains show Mg concentrations of 0.69-0.78 mol % $MgCO_3$ (equivalent to 1661-1874 ppm Mg) and 216-332 ppm Sr.

An early isopachous, fibrous cement surrounds ooid grains (Figure 4 e, f). 3D SEM analysis (Figure 6) shows it can be up to 100 µm thick with individual crystals being between 10-20 µm wide. Crystal terminations appear to be flat (Figure 6). Mg concentrations range from 0.76 – 1.46 mol % $MgCO_3$ (Figure 7), equivalent to 1820 – 3503 ppm Mg (Figure 8). Sr concentration ranges from 211 – 962 ppm (Figures 7, 8).

Much of the remaining intergranular porosity is filled by syntaxial calcite overgrowths on echinoderm fragments and finely crystalline drusy or sparry intergranular calcite cements. Oomouldic porosity is partially filled by sparry low-Mg calcite which has both low Mg (0.6 – 1.03 mol % $MgCO_3$, equivalent to 1434-2480 ppm Mg) and Sr (56-84 ppm) concentrations (Figure 7).

BSEM study shows that minor celestine ($SrSO_4$, often Ba-rich, Figure 4b) occurs in many samples with trace amounts of Sr-rich barite and strontianite. Several layers of dolomite also occur within the succession (Figure 2) and most of these contain celestine, barite or both.

$\delta^{18}O$ and $\delta^{13}C$ values of 20 representative limestones, bioclastic sandstones and calcite cemented sandstones were obtained ( -6.0 to -8.9‰ VPDB and -3.1 and +1.8 ‰ VPDB

121 respectively, Figure 2). Two excursions to positive $\delta^{13}C$ values are found (Figure 2), the first
122 confirmed by two samples at ~50 m above the base of the Al Bashair (+0.8 ‰), the second
123 excursion occurring from ~140 to 180 m (+1.8 ‰). There is no statistically significant
124 correlation at any stratigraphic depth between $\delta^{18}O$ and $\delta^{13}C$, even at a low confidence level
125 (n = 19, r = 0.18).

126

127 **Discussion**

128 **Primary Mineralogy**

129 *High- Mg Calcite*

130 Tucker (1990) suggests that microdolomite inclusions and retention of some Mg in the
131 lattice (LMC typically has less than 0.5 mol % $MgCO_3$) are evidence of a HMC precursor. The
132 radial ooids in the LAB contain both microdolomite inclusions and relatively high $MgCO_3$
133 (1.19-1.91 mol %). It is therefore suggested that they were originally HMC. The most
134 altered fibrous marine calcite cements from the Devonian of the Western Canada and
135 Canning Basins (Carpenter et al., 1991, Figure 8) and Pennsylvanian former HMC cements
136 (Davies, 1977) have similar compositions.

137 *Aragonite*

138 Sandberg (1983) suggested that the most reliable indicators of an aragonite precursor for
139 cements include square-ended crystal terminations and enhanced Sr content. Square-
140 ended crystal terminations are observed in the fibrous, isopachous cements in the LAB and
141 Sr concentrations up to 962 ppm.

Modern aragonite cements mostly have less than a few 100 ppm Mg (Dickson, 2014) but some (e.g. Holocene aragonite cements from Eniwetak atoll, Carpenter et al., 1991, Figure 8b) contain higher levels, similar to the 2000-3500 ppm Mg recorded here. Although Dickson (2014) reports that some HMC cements have elevated Sr concentrations (600 – 1800 ppm), many HMC cements have lower Sr than the maximum recorded here (e.g. Holocene abiotic HMC of Carpenter and Lohman, 1992, Figure 8a). Given the morphology and composition of the fibrous cements, it is suggested that they were originally aragonite.

For aragonite grains, Sandberg (1983) suggested that evidence of an originally aragonitic mineralogy included recrystallization by a relatively coarse cross-cutting calcite mosaic and an enhanced Sr content. Others (e.g. Tucker, 1992, Lehrmann et al, 2012) included oomouldic porosity although Sandberg (1983) suggested that this is unreliable.

The crystal size of neomorphosed coated grains in the LAB is small and Sr content is relatively low (216-332 ppm). However redistribution of Sr cannot be ruled out given their age and the presence of Sr-bearing minerals (e.g. celestine). It is possible that they were originally composed of aragonite.

**Controls on mineralogy**

Many factors are believed to affect the mineralogy of inorganic carbonates precipitated from seawater (e.g. Burton and Walter, 1987; Stanley et al., 2010, Lee and Morse, 2010; Bots et al., 2011, Balthasar and Cussack, 2015).

*Seawater mMg:Ca*

The mMg:Ca ratio of seawater is thought to be one of the main controls on whether aragonite or calcite seas prevail, with low Mg calcite forming at seawater mMg:Ca <1, marginally high Mg calcite forming between 1 and 2, and high Mg-calcite or aragonite at 2 to 5.2 (e.g. Stanley et al., 2010). The widely quoted mMg:Ca for Cambrian seawater ranges from c. 0.5 -0.8 (e.g. Stanley et al., 2010, Figure 1) implying inorganic LMC precipitation. Arvidson et al., (2006) however suggested that it could have been c. 1.2, based on geochemical modelling.

*$pCO_2$*

Lee and Morse (2010) showed that a critical region, where the effects of $pCO_2$ and alkalinity are important, is where the mMg:Ca is between 1 and 2. At a mMg:Ca of 1.2, they demonstrated that aragonite could precipitate if $pCO_2$ is over c. 2500 µatm (at alkalinities < 10 mM) as it would have been in the late Cambrian (e.g. Berner, 2006). *Temperature*

Balthasar and Cussack (2015) suggested that at a mMg:Ca ratio of 1.5 and at 30 °C aragonite will precipitate directly from seawater, with exclusive LMC precipitation only occurring at relatively low temperatures (< 21 °C) and mMg:Ca < 1. Earlier experimental work by Burton and Walter (1987) also showed that higher temperatures favoured the precipitation of aragonite and HMC.

*The SPICE*

The LAB-UAB boundary is not only marked by a change in lithology (Figure 2) but also a change to slightly positive $\delta^{13}C$ values. This is tentatively interpreted as the SPICE event, occurring at a stratigraphic height of around 150 m above the base of the Al Bashair Fm (Figure 2). Indeed, if a correction factor of +3.5‰ is added (Figure 9), the curve lies directly

over that from the neighboring regions of China and Kazakhstan (Saltzman et al., 2000, Figure 9).

Several authors (e.g. Saltzman et al., 1998, 2000; Gill et al., 2011) report a global transgression in the basal Furongian as the SPICE is approached, with a small (~ 25m) regression coincident with the peak of the SPICE excursion. A similar pattern of transgression followed by regression is seen in the Al Bashair Fm. During the SPICE, enhanced burial/preservation of organic matter created a positive shift in $\delta^{13}C$ (e.g. Brasier, 1993, Saltzman, 2000, Gill et al., 2011). Processes such as these are common during times of warmer seas and reduced thermohaline circulation (e.g. Mackenzie et al., 2000).

Aragonite and HMC could therefore have precipitated during the SPICE interval from warm seawaters with a mMg:Ca of 1.2, under high $pCO_2$ conditions.

**Global trends**

The ooids in the early Furongian Johns Wash Limestone, Utah (Figure 3f) have been interpreted as being originally aragonitic (e.g. Conley, 1977) along with ooids from the Petit Jardin and Berry Head Fms., Newfoundland (Chow and James, 1987 a and b), the Open Door Fm., Wyoming (Martin et al., 1980) and unidentified ooids from the late Cambrian (Wilkinson et al., 1984).

Stable isotope data have been published for two of these units. The Johns Wash Limestone (Brasier, 1993) and the Petit Jardin Fm., Newfoundland (Saltzman et al., 2004) have been shown to be coincident with the SPICE signal. This implies that aragonite/HMC precipitation

and the link with the SPICE observed during deposition of the Al Bashair Fm. was not just a phenomenon local to an area of Gondwana but also occurred in Laurentia (Figure 10).

## Conclusions

Although aragonite seas have been reported in the early Cambrian, until now it has been believed that calcite seas characterized Stage 5 onwards (Table 1). Possible evidence of a transient aragonite sea (capable of primary inorganic aragonite and HMC precipitation) in the early Furongian however has been obtained from the Huqf High, Oman. This is in the form of square-ended fibrous cements with elevated Sr contents (interpreted as originally being aragonitic) and possible aragonitic ooids (e.g. oomouldic porosity). Variable amounts of Sr-rich cements (e.g. celestine) are found. Radial ooids also occur which are believed to have originally been composed of HMC, another characteristic of aragonitic seas. Reports of former aragonitic ooids occur in the literature from the Johns Wash Limestone, Utah, (e.g. Conley, 1977), the Petit Jardin and Berry Head Fms., Newfoundland (Chow and James, 1987 a and b), the Open Door Fm., Wyoming (Martin et al., 1980) and unidentified deformed ooids from the late Cambrian (Wilkinson et al, 1984), suggesting a global phenomenon.

The precipitation of these phases occurred prior to and during the SPICE, a time which may have reflected warmer oceanic conditions. Aragonite precipitation could be accounted for if mMg:Ca was c. 1.2 as suggested by Arvidson et al. (2006), $pCO_2$ values were above 2500 µatm (Lee and Morse, 2010) and precipitation occurred in warm waters (Balthasar and Cussack, 2015). The +4 to +5‰ shift in $\delta^{13}C$ values documented here is similar to the SPICE identified elsewhere (e.g. Saltzman et al., 2000). This helps verify the age of the Al Bashair

Fm. and provides evidence of synchronous events on both Laurentia and Gondwana. Seawater chemistry in the late Cambrian is poorly constrained and we concur with Kiessling (2015) and Balthasar and Cusack (2015) that 'gray' or 'fuzzy' zones exist. Transient aragonite seas are likely to have existed.

**Acknowledgements**

Fieldwork and sampling was funded by Petroleum Development Oman during S. Al Marjibis's Ph.D. Their help is gratefully acknowledged. We also thank colleagues at the University of Aberdeen, Julie Dougans (SUERC) for assisting with stable isotope analysis and Dr. Richard Hinton (EIMF ) for assistance with ion microprobe analysis. Profs. Kiessling, Tucker, Bosence, Coleman, Dr. Dickson and an anonymous reviewer are thanked for their helpful and encouraging comments.

**References**

Al Marjibi, S., 2011. Unravelling the depositional environments within the lower Andam Group (Al Bashair Formation, Late Cambrian) of north-central Oman. Unpublished Ph.D. thesis, University of Aberdeen.

Arvidson, R.S., Mackenzie, F.Y. and Guidry, M., 2006. MAGic: A Phanerozoic model for the geochemical cycling of major rock-forming components. *Am. Jour. Sci.,* **306**, 135–190.

Balthasar, U. and Cussack, M., 2015. Aragonite-calcite seas—Quantifying the gray area. *Geology*, **43**, 99–102.

249 Berner , R.A., 2006. GEOCARBSULF: A combined model for Phanerozoic atmospheric $O_2$ and
250 $CO_2$. *Geochi. Cosmochim. Acta*, **70**, 5653–5664.

251 Bots, P, L.G. Benning, L.G.,, Rickaby, R.E.M. And Shaw,S., 2011. The role of $SO_4^{2-}$ in the switch
252 from calcite to aragonite seas. *Geology*, **39**, 331-334.

253 Brasier, M.D., 1993. Towards a carbon isotope stratigraphy of the Cambrian System:
254 potential of the Great Basin succession. *Geo. Soc. Lond. Spec. Pub.,* **70**, 341–350.

255 Burton, E.A. And Walter, L.M.,1987. Related precipitation rates of aragonite and Mg calcite
256 from seawater – temperature or carbonate ion control? *Geology*, **15**, 111-114.

257 Carpenter, S. J. and Lohmann, K.C., 1992. Sr /Mg ratios of modern marine calcite: Empirical
258 indicators of ocean chemistry and precipitation rate. *Geochim. Cosmochim. Acta*, **56**, 1837-
259 1849.

260 Carpenter S.J., Lohmann, K.C., Holden, P., Walter, L.M., Huston, T.J. and Halliday, A.N., 1991.
261 $\delta^{18}O$ values, $^{87}Sr/^{86}Sr$ and Sr/Mg ratios of Late Devonian abiotic marine calcite: Implications
262 for the composition of ancient seawater. *Geochim. Cosmochim. Acta*, **55**, 1991-2010.

263 Chow, N. and James, N.P., 1987a. Facies specific calcitic and bimineralic ooids from Middle
264 and Upper Cambrian platform carbonates, Western Newfoundland, Canada. *Jour. Sed. Pet.*,
265 **57**, 907-921.

266 Chow, N. and James, N.P., 1987b. Cambrian Grand Cycles: A northern Appalachian
267 perspective. *Geol. Soc. Am. Bull.*, **98**, 418-429.

268 Conley, C. D., 1977. Origin of distorted ooliths and pisoliths. *Jour. Sed. Pet.*, **47**, 554-564.

Davies, G.R., 1977. Former magnesian calcite and aragonite submarine cements in upper Paleozoic reefs of the Canadian Arctic: A summary. *Geology*, **5**, 11-15.

Demicco, R.V., Lowenstein, T.K., Hardie, L.A. and Spencer, R.J., 2005. Model of seawater composition for the Phanerozoic. *Geology*, **33**, 877–880.

Dickson, J.A.D., 2014. *Marine Beachrocks*. Carbonate Diagenesis Ltd., 41pp.

Droste, H., 1997. Stratigraphy of the lower Palaeozoic Haima Supergroup of Oman. *GeoArabia*, **2**, 419-472.

Elrick, M., Rieboldt, S., Saltzman, M, And Mckay, R.M., 2011. Oxygen-isotope trends and seawater temperature changes across the Late Cambrian Steptoean positive carbon-isotope excursion (SPICE event). *Geology*, **39**, 987–990.

Forbes, G. A., Jansen, H.S.M. and Schreurs, J., 2010. *Lexicon of Oman subsurface stratigraphy*. GeoArabia Spec. Publ. **5**.

Füchtbauer, H. and Hardie, L.A., 1976. Experimentally determined homogeneous distribution coefficients for precipitated magnesian calcites: application to marine carbonate cements. *Geol. Soc. Am. Abstracts Program*, **8**, 877.

Füchtbauer, H. and Hardie, L.A., 1980. Comparison of experimental and natural magnesian calcites. *Int. Assoc. Sedimentol.*, *Bochum, Germany,* 167–169.

Gill, B.C., Lyons, T.W., Young, S.A., Kump, L.R., Knoll, A.H. And Saltzman, M.R., 2011. Sulphur isotope evidence for widespread euxinia in the Later Cambrian ocean. *Nature*, **469**, 80-83.

James, N.P. and Klappa, C.F., 1983. Petrogenesis of Early Cambrian reef limestones, Labrador, Canada. *Jour. Sed. Pet.*,, **53**, 1051-1096.

290 Kiessling, W., 2015. Fuzzy seas. *Geology*, **43**, 191-192.

291 Landing, E., 1983. Highgate Gorge: Upper Cambrian and Lower Ordovician

292 continental slope deposition and biostratigraphy, northwestern Vermont.

293 *Jour. Paleo*, **57**, 1149–1187.

294 Lee, J. and Morse, J.W., 2010. Influences of alkalinity and $pCO_2$ on $CaCO_3$ nucleation from

295 estimated Cretaceous composition seawater representative of ''calcite seas''. *Geology*, **38**,

296 115-118.

297 Lehrmann, D.J., Minzoni, M., Li, X., Yu, M., Payne, J.L., Kelley, B.M., Schaal, E.K. and Enos,

298 P., 2012. Lower Triassic oolites of the Nanpanjiang Basin, south China: Facies architecture,

299 giant ooids, and diagenesis—Implications for hydrocarbon reservoirs. *Am. Assoc. Pet. Geol.*

300 *Bull.*, **96**, 1389–1414.

301 Mackenzie, F. T., Ver, L.M., and Lerman, A., 2000. Coastal-Zone Biogeochemical Dynamics

302 under Global Warming. *Internat. Geol. Rev.*, **42**, 193-206.

303 Martin, W.D., Fischer, H.J., Keogh, R.J. and Moorse, K., 1980. The petrology of the

304 limestones in the Upper Gros Ventre and Gallatin Limestone Formations (Middle and Upper

305 Cambrian) Northwestern Wind River Basin, Wyoming. *Stratigraphy of Wyoming 31$^{st}$ Annual*

306 *Field Conference Guidebook*, 37-51.

307 Morse, J.W., Wang, Q., And Tsio, M.Y., 1997. Influences of temperature and Mg:Ca Ratio On

308 $Caco_3$ Precipitates From Seawater. *Geology*, **25**, 85–87.

309 Peng, S., Babcock, L. and Cooper, R. A., 2012. The Cambrian Period, In: *The Geologic Time*

310 *Scale 2012* (F.M. Gradstein, J.G. Ogg, M. Schmitz and G. Ogg eds.) Elsevier, 437- 488.

311 Ries, J.B., 2009. Effects of secular variation in seawater mMg:Ca ratio (calcite-aragonite seas)
312 on $CaCO_3$ sediment production by the calcareous alga *Halimeda, Penicillus* and *Udotea* –
313 evidence from recent experiments and the geological record. *Terra Nova*, **21**, 323-339.

314 Saltzman, M.R., Clinton, A.C., Runkel, A.C., Runnegar, B., Stewart, M.C. and Palmer, A.R.,
315 2004. The late Cambrian SPICE ($\delta^{13}C$) event and the Sauk II-Sauk III regression: New
316 evidence from Laurentian basins in Utah, Iowa and Newfoundland. *Jour. Sed. Res.*, **74**, 366–
317 377.

318 Saltzman, M.R., Ripperdan, R.L., Brasier, M.D., Lohmann, K.C., Robison, R.A, Chang f, Shanchi
319 Peng, W.T., Ergaliev, E.K., Runnegar, B., 2000. A global carbon isotope excursion (SPICE)
320 during the Late Cambrian: relation to trilobite extinctions, organic-matter burial and sea
321 level. *Palaeogeography, Palaeoclimatology, Palaeoecology*, **162**, 211.

322 Saltzman, M.R., Runnegar, B. and Lohmann, K.C., 1998. Carbon isotope stratigraphy of
323 Upper Cambrian (Steptoean Stage) sequences of the eastern Great Basin: record of a global
324 oceanographic event. *Geol. Soc., Am.*, **110**, 285–297.

325 Sandberg, P.A., 1983. An oscillating trend in Phanerozoic nonskeletal carbonate mineralogy.
326 *Nature*, **305**, 19-22.

327 Stanley, S.M., Ries, J.B. and Hardie, L.A., 2010. Increased production of calcite and slower
328 growth for the major sediment-producing alga Halimeda as the Mg/Ca ratio of seawater is
329 lowered to a ‘‘calcite sea’’ level. *Jour. Sed. Res.*, **80**, 6–16.

330 Tucker, M.E., 1992. The Precambrian-Cambrian boundary: Seawater chemistry, ocean
331 circulation and nutrient supply in metazoan evolution, extinction and biomineralization.
332 *Jour. Geol. Soc. Lond.*, **149**, 655-668.

333 Vizan, H., Turner, P., Millison, J.S. and Ixer, R.A., 2009. Palaeomagnetism of the Mahatta
334 Humaid Group (Cambrian-Early Ordovician, Oman), including a re-interpretation of previous
335 Neoproterozoic palaeomagnetic data. *GeoArabia*, **14**, 71-96.

336 Wilkinson, B.H., Buczynski, C. and Owen R.M., 1984. Chemical control of carbonate phases:
337 Implications from Upper Pennsylvanian Calcite-Aragonite ooids of Southeastern Kansas.
338 *Jour. Sed. Pet.*, **54**, 932-947.

339 Wood, R.A., Zhuravlev, A.Y. and Chimed Tseren, A., 1993. The ecology of Lower Cambrian
340 buildups from Zunne Arts, Mongolia: Implications for early metazoan reef evolution.
341 *Sedimentology*, **40**, 829-858.

342 Zhuravlev, A. Y. and Wood, R.A., 2008. Eve of biomineralization: Controls on skeletal
343 mineralogy. *Geology*, **36**, 923-926.

344

345 **Figure and Table Captions**

346

347 **Figure 1** – The relationship between seawater mMg:Ca and primary marine mineralogy
348 through the Phanerozoic (Stanley et al, 2010). Star is the mMg:Ca ratio of Arvidson et al.,
349 (2006). A = aragonite sea, C = calcite sea.

350

351 **Figure 2** - Summary of the sedimentology of the Lower Al Bashair Fm. (LAB) and
352 petrographic features of the oolitic grainstones. Height is from the base of the Al Bashair
353 Fm. in metres. Red-dashed line is interpreted boundary between the lower Al Bashair (LAB)
354 and upper Al Bashair (UAB). Lithology has been summarized as shown, with a relative grain-
355 size curve (finer to the left).The presence of relict coated grains and radial ooids are shown
356 as horizontal lines. All whole rock $\delta^{18}O$ and $\delta^{13}C$ VPDB data are from limestones, bioclastic
357 sandstones or, in two cases, calcite cemented sandstones (C) to determine the effect of
358 diagenesis.

359

360 **Figure 3** – Plane-polarized images (A-E) of Al Bashair Formation carbonates and siliciclastics.
361 Height above base Al Bashair Fm shown and (F) JWL - Johns Wash Limestone, House Range,
362 Utah.

363 A) Oolitic grainstone with radial cortices (R). Intergranular porosity filled by early,
364 isopachous, fibrous cement (arrow) followed by sparry calcite (C)Ooid nuclei of variable
365 composition including occasional quartz grains (Q). Scale bar as shown.

B) Relict coated grainstone with abundant oomouldic porosity (blue). Ooids are larger than in the example shown in (A). Isopachous, fibrous cements (arrow) surround grains with the remaining intergranular porosity filled by drusy to sparry calcite (C). Scale bar as shown.

C) Peloidal bioclastic grainstone containing trilobite (T) and echinoderm (E) fragments. A glauconite grain is circled. Limited porosity. Scale bar as shown.

D) Fine grained porous bioclastic sandstone containing elongate brachiopod (arrow) fragments. Porosity shown in pale blue. Scale bar as shown.

E) Fine grained porous sandstone. No bioclastic fragments are present. Porosity is shown in pale blue. Scale bar as shown.

F) Recrystallised oolitic grainstone, Johns Wash Limestone, House Range, Utah. Ooid grains (O) are of a similar size to the relict coated grains in the Al Bashair Fm. Sample JWL2 from the Martin Brasier Collection, University of Oxford. Scale bar as shown.

**Figure 4** – Plane-polarized images (A, E, F) and back-scatter scanning electron images (B-D) of Al Bashair Formation carbonates. Height above base Al Bashair Fm shown.

A) Relict coated grain grainstone showing oomouldic porosity filled to varying degrees: porosity unfilled (1), porosity partially filled by sparry calcite (2), porosity totally filled by sparry calcite (3) and neomorphosed coated grains (4). Ion probe data indicates that the mould fill calcite (0.6 – 1.1 mol % $MgCO_3$, < 100 ppm Sr) is distinct in composition from the intergranular calcite (0.9 – 1.6 mol% $MgCO_3$, 100 – 500 ppm Sr) . Scale bar as shown.

B) Relict coated grainstone with abundant oomouldic porosity (dark grey) partially filled by celestine (white). Scale bar as shown.

C) Well cemented oolitic grainstone. Ooids are dark grey (1.19 – 1.91 mol % $MgCO_3$, equivalent to 2866 – 4599 ppm Mg). In PPL, these ooids show a radial fibrous structure. Scale bar as shown.

D) Detail of radial ooid in Figure 4C. Microdolomite inclusion (arrow) within grain. Scale bar as shown.

E-F) Relict coated grainstone showing well developed isopachous, fibrous cements (arrow) surrounding oomoulds (O). Scale bar as shown.

**Figure 5** – Grain size data collected from Al Bashair formation oolitic grainstones. Grains in the relict coated grainstones (110.25 m and 125.75 m above the base Al Bashair Fm.) are larger than those in the radial oolitic grainstones (4.25 m and 138 m above the base Al Bashair Fm.). The large Al Bashair Fm. coated grains and those of similar size in the Johns Wash Limestone (Figure 3F) are believed to have originally been aragonitic while the smaller radial ooids are believed to have been originally HMC.

**Figure 6 –** Secondary electron images of the fibrous isopachous cements (F) taken at different magnifications. Note square crystal terminations (white circles). O – oomouldic porosity. 110.25 m above base Al Bashair Fm.

406 **Figure 7 –** Ion microprobe data (Mg and Sr) collected for different grain and cement phases
407 in the Al Bashair Fm. IEG – intergranular porosity. AB20 - 110.25 m above base Al Bashair
408 Fm., M22 - 4.25m above base Al Bashair Fm.

409

410 **Figure 8** – Ion microprobe data (Mg and Sr). (A) Al Bashair radial ooids and fibrous cements
411 (this study) compared to radial axial fibrous calcite (RAFC) samples from the Canning Basin
412 and Western Canada Basin, Devonian (Carpenter et al., 1991). Black dashed arrow is the
413 line of best fit (y=0.027x + 47) for Holocene abiotic marine calcite (Carpenter and Lohman,
414 1992). (B) Comparison of unaltered Holocene aragonite cements (Enewetak Atoll,
415 Carpenter et al., 1991) and Al Bashair fibrous cements (this study).

416

417 **Figure 9** - $\delta^{13}C$ data for the Al Bashair Fm. (this study) plotted against the data of Saltzman et
418 al. (2000) from China. The two circled Al Bashair Fm. datapoints are from calcite cemented
419 sandstones which are $3.5^{o}/_{oo}$ lighter in $\delta^{13}C$ than bioclastic samples at a similar level. This
420 implies a diagenetic effect and when a correction factor of $+3.5^{o}/_{oo}$ is added to the Al
421 Bashair Fm. data, the trend lies directly above that of the data from China.

422

423 **Figure 10 –** Plate reconstruction for the late Cambrian (Peng et al., 2012) showing
424 occurrences of Furongian aragonite and HMC. 1 – Al Bashair Formation, 2 – Petit Jardin
425 Formation (Chow and James, 1987 a and b), 3 - Johns Wash Limestone, Utah (Conley, 1977)
426 ad 4 - the Open Door Fm., Wyoming (Martin et al., 1980). All are in tropical locations. Red -
427 landmass, blue – shallow shelf.

**Table 1**– Stratigraphy of the Ediacaran-Ordovician in Central Oman showing the ages of the Formations within the Mahatta Humaid (Miqrat Fm.) and Andam Groups (Al Bashair and Barik Fms., after Forbes et al., 2010) and the composition of marine cements and ooids during the Ediacaran to Early Ordovician from global datasets. Stage/Age nomenclature and age (Ma) of Cambrian based on that of Peng et al. (2012). N/D = no data available.

**Table 2** – Relationship between stratigraphic terminology used for the Cambrian in different parts of the globe and related to trilobite zones based on Chow and James (1987 a and b) and Elrick et al. (2011). Evidence for aragonite and high-Mg calcite precipitation highlighted in grey from this and the studies listed in Table 1.

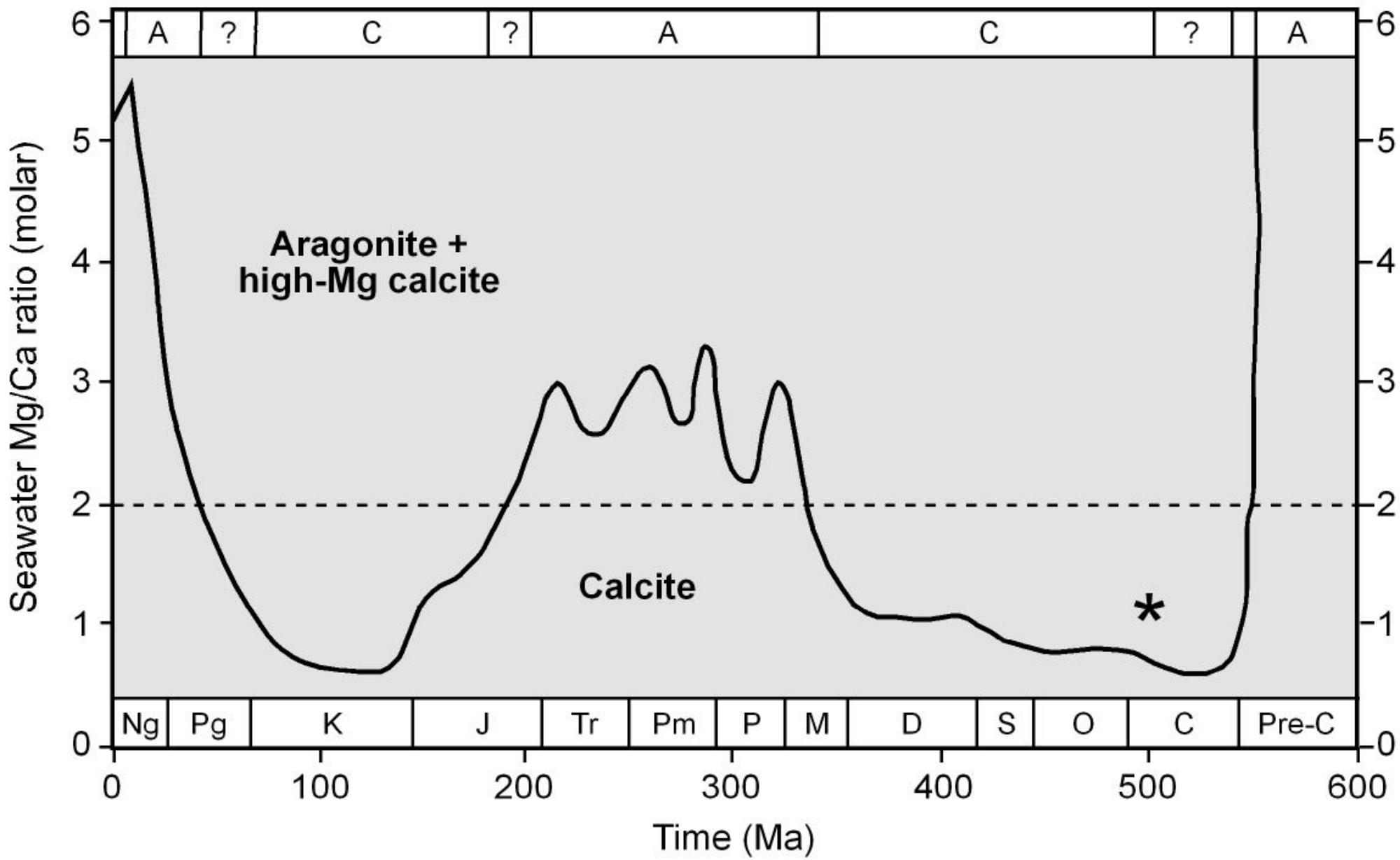
A
?
C
?
A
C
?
A
Aragonite +
high-Mg calcite
Calcite
*
Ng
Pg
K
J
Tr
Pm
P
M
D
S
O
C
Pre-C
Seawater Mg/Ca ratio (molar)
Time (Ma)
0
1
2
3
4
5
6
0
100
200
300
400
500
600

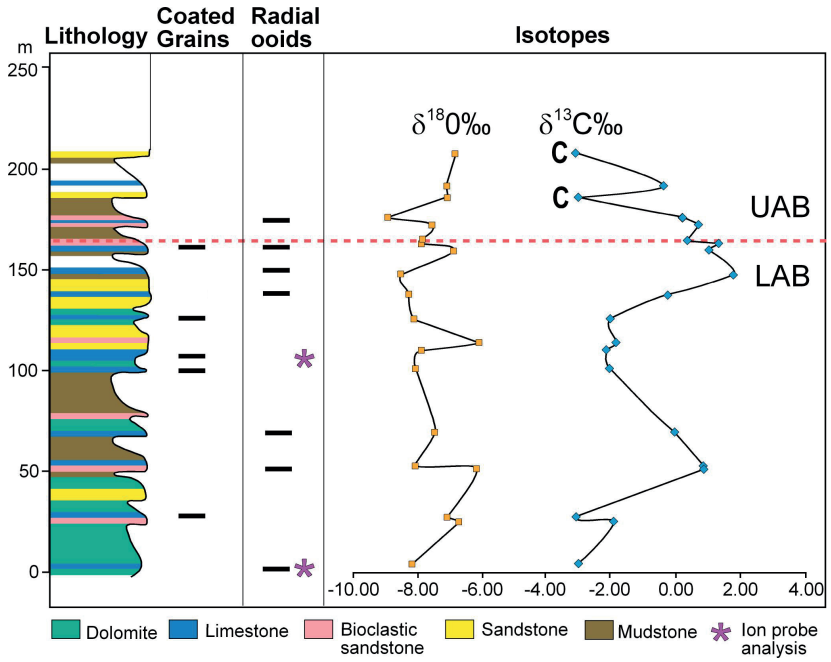
Lithology
Coated Grains
Radial ooids
Isotopes
m
250
200
150
100
50
0
δ18O‰
δ13C‰
C
C
UAB
LAB
-10.00
-8.00
-6.00
-4.00
-2.00
0.00
2.00
4.00
Dolomite
Limestone
Bioclastic sandstone
Sandstone
Mudstone
Ion probe analysis

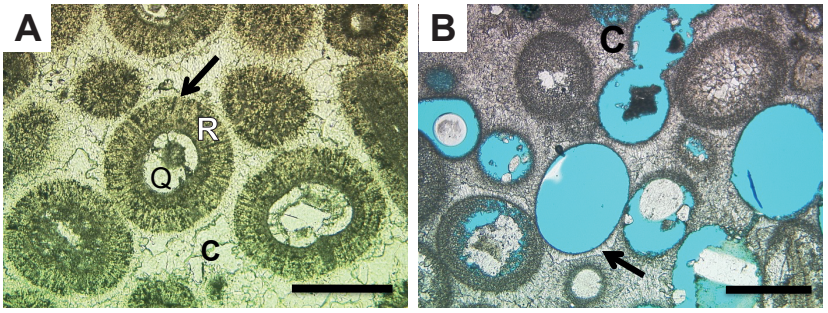


4.25m 250 μm 110.25m 500 μm

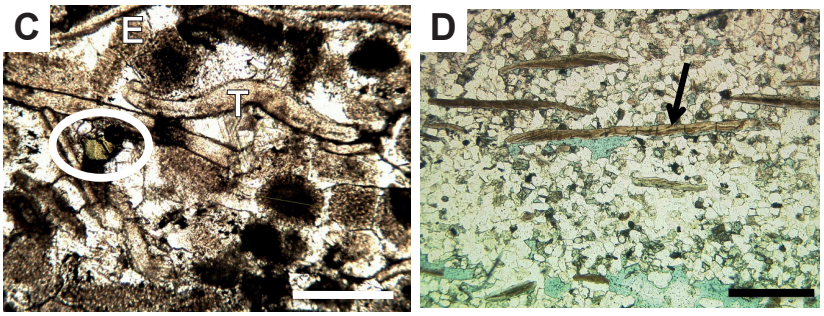


27.25m 250 μm 116.5m 500 μm

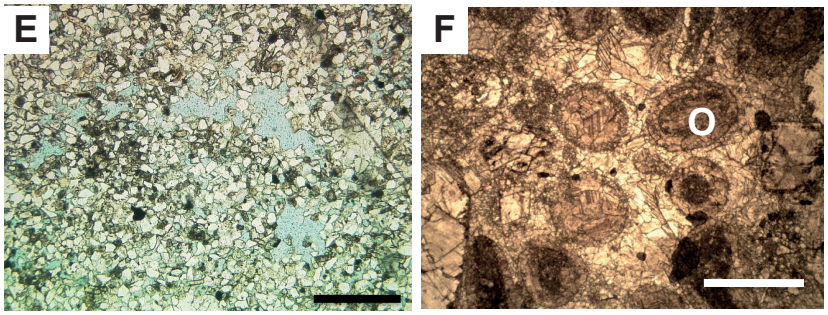


113.95m 500 μm JWL 800 μm

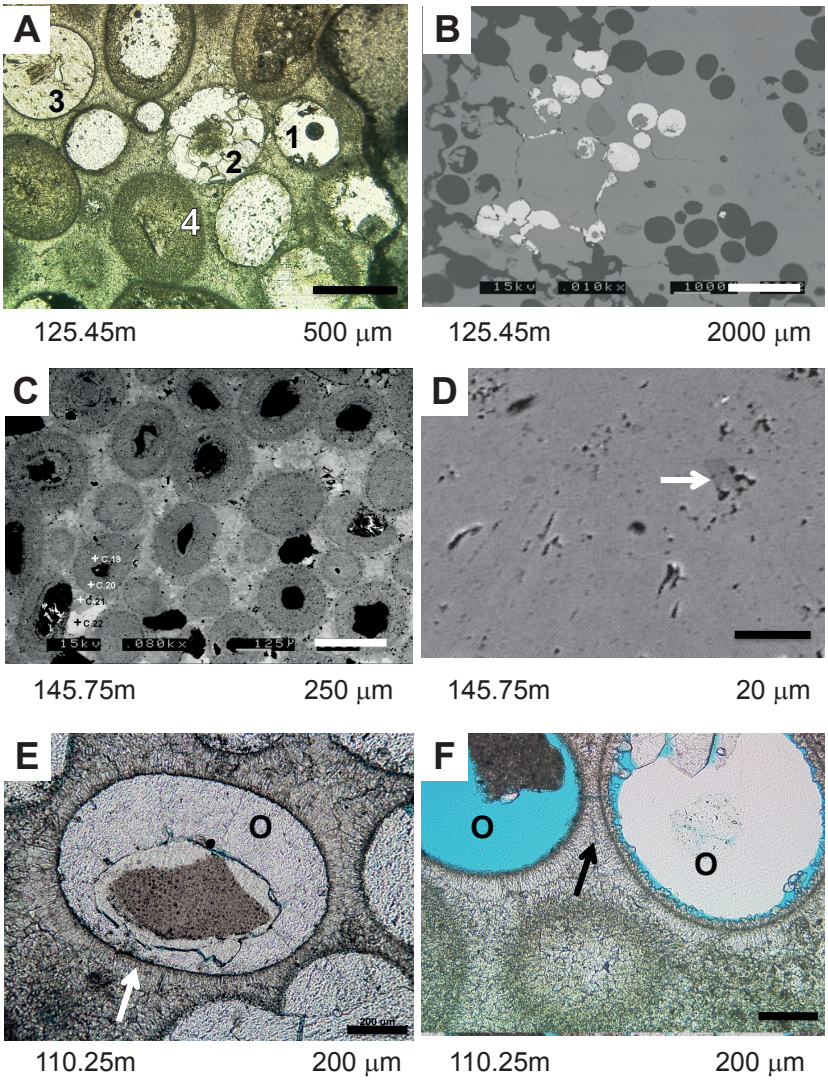
A
3
1
2
4
125.45m
500 μm
B
125.45m
2000 μm
C
145.75m
250 μm
D
145.75m
20 μm
E
O
110.25m
200 μm
F
O
O
110.25m
200 μm

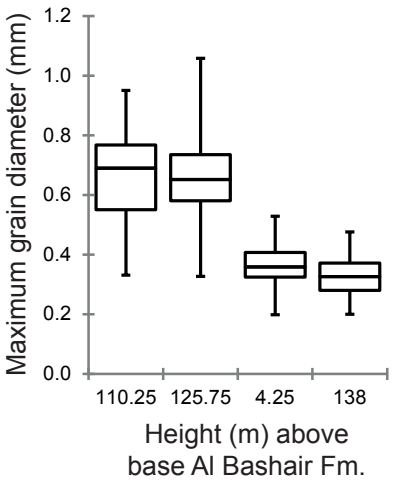
Maximum grain diameter (mm)
1.2
1.0
0.8
0.6
0.4
0.2
0.0
110.25
125.75
4.25
138
Height (m) above
base Al Bashair Fm.

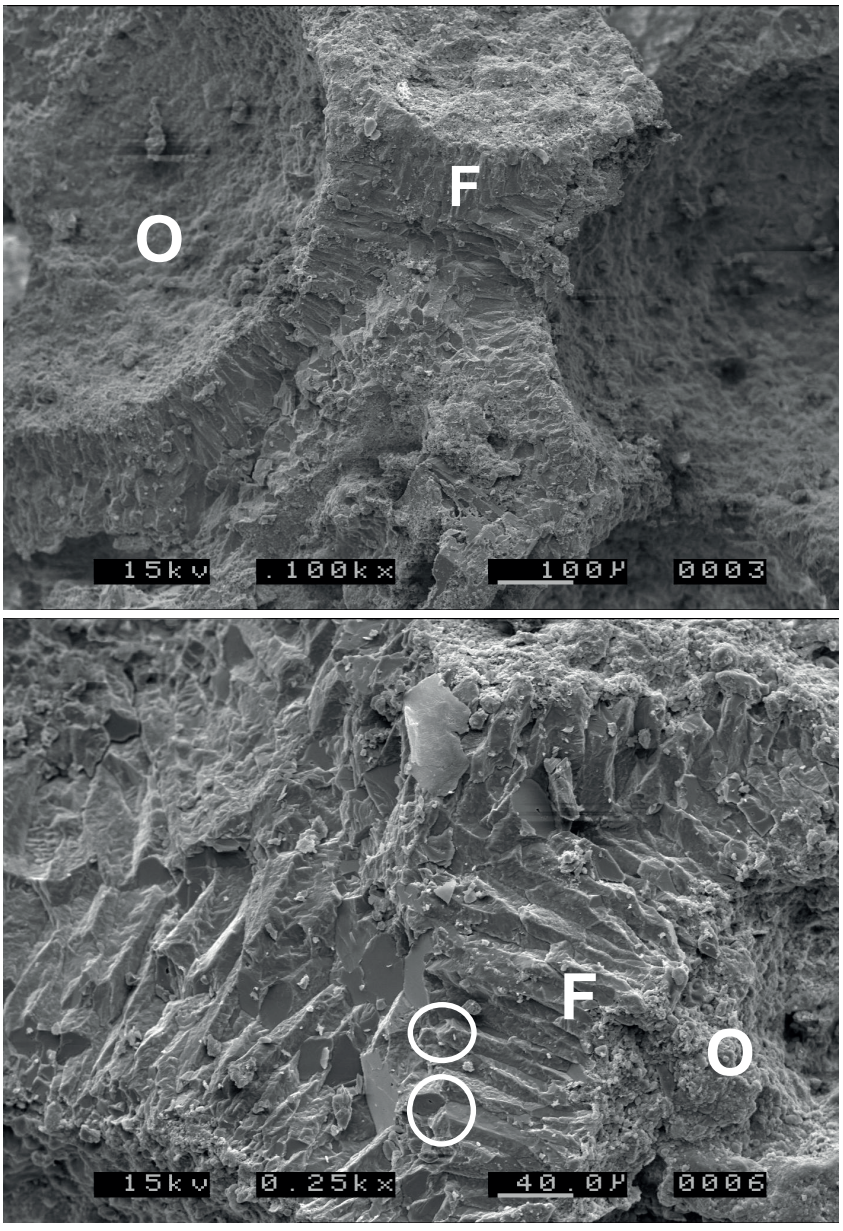
O
F
15kv .100kx 100µ 0003
F
O
15kv 0.25kx 40.0µ 0006

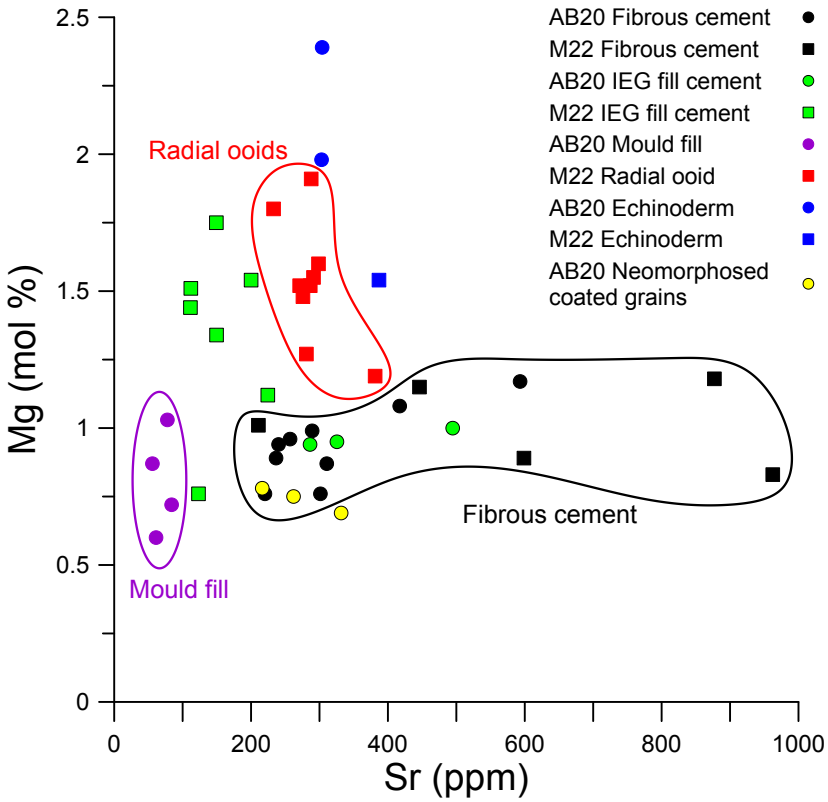
AB20 Fibrous cement
M22 Fibrous cement
AB20 IEG fill cement
M22 IEG fill cement
AB20 Mould fill
M22 Radial ooid
AB20 Echinoderm
M22 Echinoderm
AB20 Neomorphosed coated grains
Radial ooids
Fibrous cement
Mould fill
Mg (mol %)
Sr (ppm)
2.5
2
1.5
1
0.5
0
0
200
400
600
800
1000

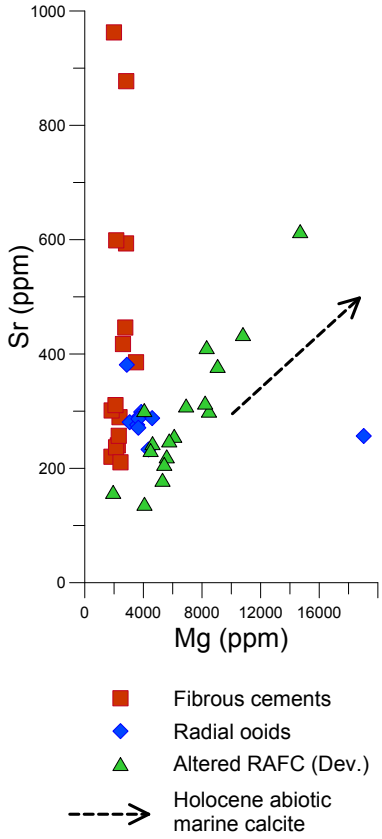
1000
800
600
400
200
0
Sr (ppm)
0
4000
8000
12000
16000
Mg (ppm)
Fibrous cements
Radial ooids
Altered RAFC (Dev.)
Holocene abiotic
marine calcite

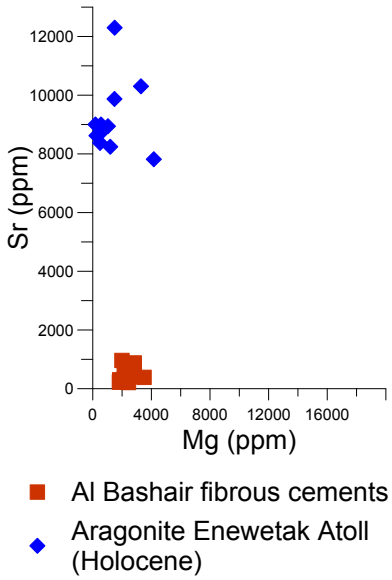
12000
10000
8000
6000
4000
2000
0
Sr (ppm)
0
4000
8000
12000
16000
Mg (ppm)
Al Bashair fibrous cements
Aragonite Enewetak Atoll (Holocene)

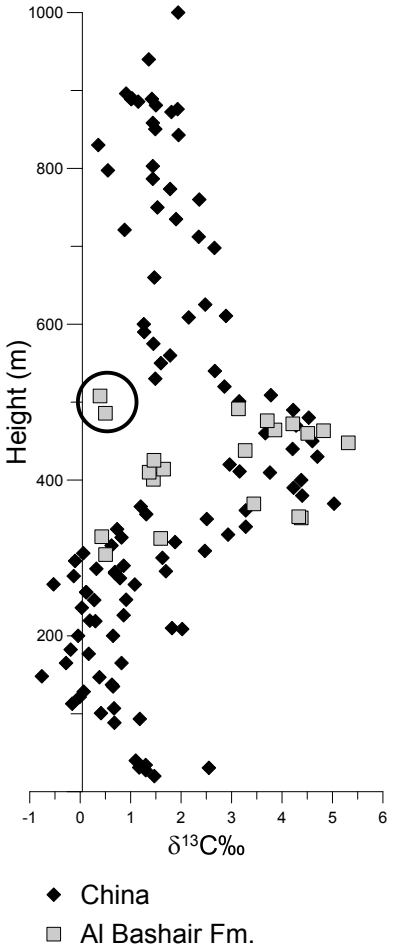
1000
800
600
400
200
Height (m)
-1
0
1
2
3
4
5
6
δ13C‰
China
Al Bashair Fm.

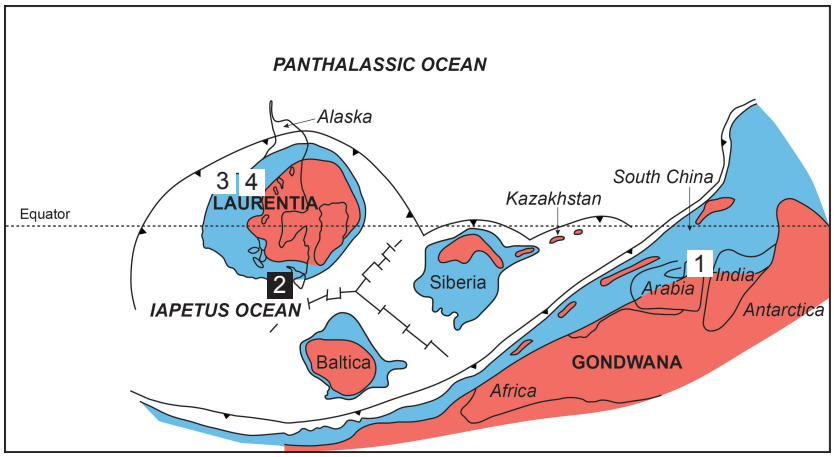
PANTHALASSIC OCEAN
Alaska
3
4
LAURENTIA
Equator
Kazakhstan
South China
1
India
Arabia
Antarctica
2
IAPETUS OCEAN
Siberia
Baltica
GONDWANA
Africa

| SYSTEM/ PERIOD | SERIES/ EPOCH | STAGE / AGE | FORMATION (OMAN) | MINERALOGY | SOURCE OF DATA |
|---|---|---|---|---|---|
| **ORDOVICIAN** | Middle | | | Calcite (LMC) | Zhuralev and Wood (2008) |
| | Early | *485.4* | | | |
| **CAMBRIAN** | Furongian | Stage 10 *489.5* | Barik | Calcite (LMC) | |
| | | Jiangshanian *494.0* | | | |
| | | Paibian *497.0* | Al Bashair | Aragonite and HMC | This study; Conley, (1977) Martin et al., (1980) Chow and James (1987 a,b) |
| | Series 3 | Guzhangian *500.5* | Miqrat | | |
| | | Drumian *504.5* | | Calcite (LMC) | Zhuralev and Wood (2008) |
| | | Stage 5 *509.0* | | N/D | |
| | Series 2 | Stage 4 *514.0* | | Aragonite and HMC | Zhuralev and Wood (2008) James and Klappa (1983) Wood et al. (1993) |
| | | Stage 3 *521.0* | | Calcite (LMC) | |
| | Terreneu-vian | Stage 2 *529.0* | | Aragonite and HMC | Tucker (1992) |
| | | Fortunian *541.0* | | | Zhuralev and Wood (2008) |
| **EDIACARAN** | | | | | |

| **SERIES/ EPOCH** | **STAGE / AGE** (Peng et al., 2012) | **STAGE / AGE NORTH AMERICA** (Peng et al., 2012) | **TRILOBITE ZONE** (Landing, 1983) |
|---|---|---|---|
| | | | |
| Furongian | Stage 10 | Sunwaptan | *Taenicephalus* |
| | Jiangshanian | | |
| | Paibian | Steptoean | *Elvinia*<br>*Dunderbergia*<br>*Aphelaspis* |
| Series 3 | Guzhangian | Marjuman | *Crepicephalus*<br>*Cedaria* |